npj | climate and atmospheric science

Article

Published in partnership with CECCR at King Abdulaziz University

https://doi.org/10.1038/s41612-025-01046-4

Summer 2024 in northern Fennoscandia was very likely the warmest in 2000 years

Mika Rantanen[1] ✉, Samuli Helama[2], Jouni Räisänen[3] & Hilppa Gregow[1]

Summer 2024 was exceptionally warm in northern Fennoscandia, with June-August mean temperatures at several long-term weather stations surpassing the long-standing record set in 1937. In this region, summer mean temperatures have been reconstructed from tree-ring proxies, which provide annually resolved and millennium-long records of past climate. Here we show, using in-situ observations and two different tree-ring reconstructions, that summer 2024 was the warmest summer in 2000 years in northern Fennoscandia. Employing an attribution method based on Coupled Model Intercomparison Project Phase 6 climate models, we further estimate that climate change increased the likelihood of this extreme season by a factor of 93 (5–95% uncertainty range 19–881) and increased the temperature an additional 2.1 °C (1.4–2.8 °C). Atmospheric circulation patterns influencing both summers 1937 and 2024 were largely similar, suggesting a comparable large-scale circulation influence. Our findings highlight the impact of climate change for the contemporary heat extremes in Fennoscandia, indicating that the warming of summer climate is emerging from its range of natural climate variability over the last two millennia.

The summer warming in Europe has been particularly pronounced compared to other land areas in the northern hemisphere mid- and high latitudes. A series of successive extreme heatwaves in recent summers in 2018[1], in 2019[2], in 2021[3], in 2022[4,5] and in 2023[6,7] have prompted researchers to investigate the causes of the disproportionate intensification of heat extremes in Europe. This has led to an emerging consensus that atmospheric circulation has contributed to the intensification of heat extremes in western Europe[8–14]. Mechanisms include changes in the jet stream[8] and more frequent inflows of warm air from Iberia and North Africa[11]. However, it remains unclear whether the changes in circulation are externally forced or represent unforced internal variability of the climate system, or both[10,14].

Given the strong warming trend in European summers, it is not surprising that summer 2024 was the warmest in European instrumental records[15]. The previous record-warm summer only aged two years and was from summer 2022, when especially the Mediterranean region experienced a dry and hot summer as a result from northward-shifted jet[16]. In summer 2024, however, the largest temperature anomalies occurred in eastern and northern Europe[17].

In northern Fennoscandia, the summer 2024 marked the warmest summer on record[18]. The region has several long-running rural weather stations that have been monitoring the weather since the late 19th or early 20th century without substantial changes in location (Fig. 1). At these stations, the summer 2024 was the warmest in history, beating thus the long-standing record from 1937 which was the warmest summer at all these stations before 2024. In the northernmost region of Finland, a record-high number of 25 hot days with maximum temperature exceeding 25 °C was observed in Utsjoki Kevo (69°46'N, 27°01'E) during the summer season, with persistent hot weather contributing to the ignition of numerous forest fires in Lapland[19].

To date, the majority of attribution studies on European heatwaves have focused on extreme heat events in western Europe[2,20–22]. Northern Europe has received comparatively less attention, likely due to the lower number of high-impact heatwaves and the weaker trend in extreme temperatures relative to western Europe[9,23]. Nevertheless, the 2018 summer heatwave in Scandinavia stands as a notable exception. This event attracted considerable interest among researchers due to its extended duration and the associated dryness[1,24,25]. Attribution analyses indicated that the warmth observed in July 2018 in Scandinavia was approximately 100 times more likely to have occurred as a result of climate change[26], with probability ratios varying according to the temporal scale selected for the event[27].

Apart from meteorological records, the recent extremes can be viewed in the context of palaeoclimatic reconstructions[28], especially those being annually resolved, dated to calendar years, and rigorously calibrated and verified against the existing instrumental observations. Tree-ring chronologies fulfil these requirements[29], and several temperature reconstructions inferred from Scots pine (*Pinus sylvestris*) tree-ring data of subfossil and modern samples have been produced also for northern Fennoscandia. The reconstructions typically covering the past 1000–2000 years are based on

[1]Finnish Meteorological Institute, Helsinki, Finland. [2]Natural Resources Institute Finland, Rovaniemi, Finland. [3]Faculty of Science, Institute for Atmospheric and Earth System Research/Physics, University of Helsinki, Helsinki, Finland. ✉e-mail: mika.rantanen@fmi.fi

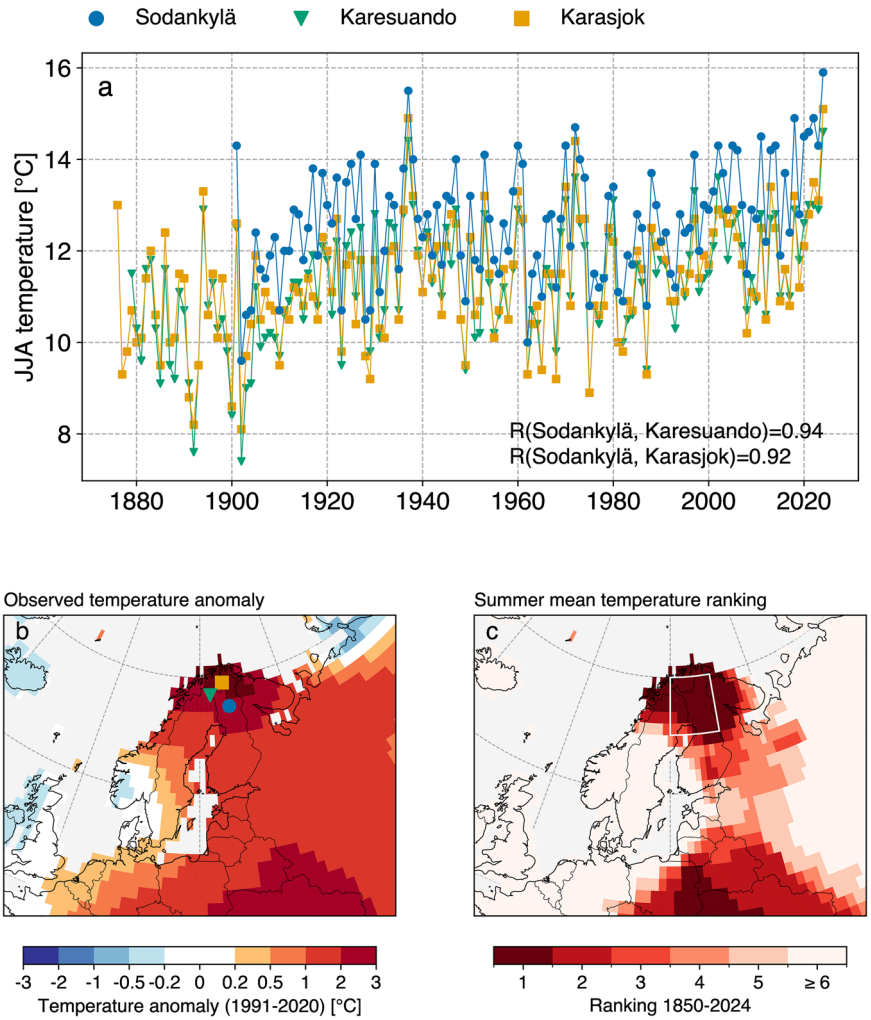

Fig. 1 | Summer 2024 was record-warm in northern Fennoscandia. a Time series of observed summer mean temperatures in Sodankylä Tähtelä, Finland (blue), Karesuando, Sweden (green) and Karasjok, Norway (orange). **b** Temperature anomaly and (**c**) ranking in summer 2024 derived from the Berkeley Earth land-only dataset. The anomaly in (**b**) is calculated relative to the 1991–2020 baseline, and the ranking in (**c**) uses the 1850–2024 time series. The markers in (**b**) depicts the station locations, and the white polygon in (**c**) depicts the domain (66°–70°N, 20°–30°E) used in Fig. 3.

maximum latewood density[30,31] or, more recently, the wood anatomy[32]. These records benefit from strong relation to summer temperatures, in comparison to more conventional data based on tree-ring widths.

These data allow comparisons with instrumental observations and place the ongoing temperature trends in a late Holocene context. Compared to several other types of palaeoclimate data, tree-ring reconstructions are not impaired by dating uncertainties or loss of high-frequency climate information but can be directly analysed with meteorological time-series. Merged with recent data of observed temperature extremes, the tree-ring records offer insights into natural climate variability long before human influence[33].

This article aims to put the recent record-warm summer 2024 in northern Fennoscandia in its long-term context by exploring two main research questions: (1) was the summer 2024 warmer than those occurred throughout the Common Era, or have there been warmer summers, for example during the Medieval Warm Period, and (2) what was the contribution of human-induced climate change to the record-warm summer in 2024? In addition to these questions, we also examine the influence of atmospheric circulation on the temperatures of summer 2024 and 1937, aiming to understand whether similar meteorological factors contributed to these two extreme summers.

Results

Instrumental and reconstructed summer temperatures in northern Fennoscandia

In this section, we present reconstructed summer mean temperature in northern Fennoscandia based on two tree-ring reconstructions: Björklund et al. [32], hereafter BJ23, for the years 850–2019 CE and Matskovsky and Helama[34], hereafter MH14, for the years −7–2010 CE. The reconstructed observations were scaled using station observations from Sodankylä Tähtelä (see Methods), and therefore they correlate well with Sodankylä station observations with Pearson correlations $R = 0.82$ for BJ23 and $R = 0.74$ for MH14 for the time periods they overlap (Fig. 2a). The in-situ observations from Sodankylä Tähtelä are also highly correlated with the observations from Karesuando and Karasjok stations, with correlation coefficients 0.94 and 0.92, respectively, as well as regionally averaged temperature in northern Fennoscandia with $R = 0.96$ (Fig. 3).

Both reconstructions exhibit considerable natural variability on various timescales. Year-to-year fluctuations are primarily driven by random weather variability, with particularly cold summers linked to volcanic forcing[35,36]. On decadal scales, solar activity and Atlantic multidecadal variability has been shown to influence summer climate in northern Fennoscandia[37]. The long-term, gradual cooling trend visible in the MH14 reconstruction (Fig. 2c) has been attributed to slow orbital changes of the Earth[38].

In the BJ23 reconstruction (Fig. 2b), the warmest 30-year period is the most recent 30-year period of the dataset, i.e., 1990–2019. According to this reconstruction, the modern warming has therefore passed the warm anomaly in the 1930–40 s, and it also appears that today's summer climate in northern Fennoscandia is substantially warmer than that of the medieval period (950–1250 CE).

In the MH14 reconstruction however, the latest available 30-year period of 1981–2010 has not yet exceeded the peak of the 1930s, and the medieval climate anomaly appears to be warmer than that of 1981–2010 (Fig. 2c). Furthermore, the warmest 30-year period is found at the beginning

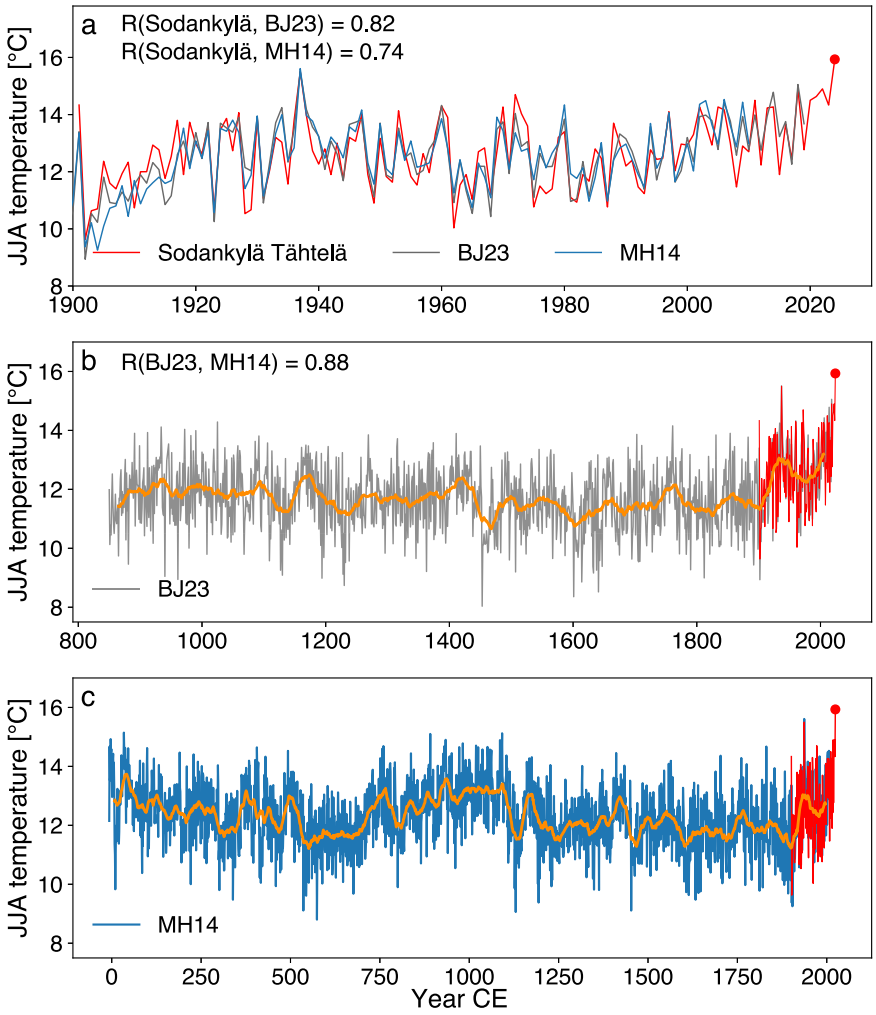

Fig. 2 | Summer 2024 temperatures in the Common Era context. a Instrumental JJA temperatures in Sodankylä (red, in-situ) shown together with BJ23 temperature reconstruction (grey) and MH14 temperature reconstruction (blue) for 1900 to present. **b** BJ23 temperature reconstruction (grey) and its 30-year moving average (orange) with instrumental JJA temperatures (red). **c** Same as (**b**), but for the MH14 reconstruction.

of the Common Era, from 27 to 56 CE. Thus, while BJ23 emphasises that the modern warming is more pronounced compared to the medieval period, in the MH14 reconstruction the modern warming does not yet emerge from the natural climate variations of the Common Era.

It is worth noting that the BJ23 reconstruction extends to 2019, thereby including the relatively warm summers from 2011 to 2019. This extended time period contributes to making the most recent 30-year period (1990–2019) the warmest in the BJ23 dataset. If the years 2011–2019 are excluded from BJ23, the warmest 30-year period shifts to 1918–1947.

In both BJ23 and MH14 reconstructions the warmest summer is 1937 with estimated mean temperatures of 15.5 °C and 15.6 °C, respectively (Fig. 2b, c and Table 1). It is evident from station observations that the warmth of summer 1937 was exceeded in 2024 not only at the Sodankylä station but also at two other long-term weather stations in northern Fennoscandia (Fig. 1) and as a regional average for northern Fennoscandia (Fig. 3). We can therefore conclude that the mean temperature in summer 2024 in northern Fennoscandia reached a level that is unparalleled in terms of natural climate variability during the last 2000 years, i.e., during the Common Era.

Nevertheless, we acknowledge that when accounting for the 95% confidence interval of the reconstructions, the upper bound for the year 34 CE in MH14 was 0.2 °C higher than the observed 2024 temperature (Fig. 4b). The reconstructed mean temperature for the year 34 CE was 15.1 °C, with a 95% confidence interval of 14.3–16.1 °C. On millennial scales, however, the Milankovitch theory suggests that orbital forcing has led to decreased summer insolation at the latitudes of our sites[39], this forcing thus gradually cooling the regional summer temperatures. Long-term trends estimated for the data constituting the reconstructions we have analysed have shown that the northern Fennoscandia has cooled at a rate of about −0.3 °C per 1000 years over the Common Era[38] (prior to 1901 CE). Later, this cooling estimate has been elaborated for different time periods and combinations of data[40,41] and more gradual summer cooling trends (around −0.13 °C per 1000 years, calculated over the middle and late Holocene) have been demonstrated for different types of Fennoscandian and Arctic proxy records, including tree-ring data[42]. To conclude, the cooling estimated from tree-ring data originally over the Common Era is likely inflated due to natural climate variations of shorter duration[42], but even the more conservative estimate (−0.13 °C per 1000 years) suggests that the reconstructed temperature in 34 CE should be considered in the light of orbital forcing. Thus, despite the greater solar insolation during the early first millennium, the summer of 2024 was still very likely warmer than any summer over the Common Era.

Impact of climate change on record-warm summer 2024 in northern Fennoscandia

In this section, we estimate the impact of climate change on the summer 2024 mean temperature in Sodankylä Tähtelä. Previously, this method has been used to attribute the effect of climate change on record-warm months in Helsinki Kaisaniemi[43], and the first version of the method was documented in the studies of Räisänen and Ruokolainen[44,45].

Combining the information from Coupled Model Intercomparison Project Phase 6 (CMIP6) climate model simulations and the observed global mean warming, the time series of summer mean temperature observations at Sodankylä Tähtelä are adjusted to represent stationary past, current and future climates, for which we use the years 1900, 2024 and 2050 (see

Methods). Here, we assume that the climate in 1900 approximately represents the preindustrial time, in the absence of anthropogenic influences.

The stationary observations (so called pseudo-observations) representing today's climate (year 2024) are shown in Fig. 5a together with the actual (non-stationary) observations. The difference between observations and pseudo-observations increases backwards in time, as the difference in global mean temperature between the present and the past increases. For 2024, the actual observations and the pseudo-observations are identical, as the pseudo-observations represent the climate of 2024. Notably, according to the pseudo-observations, the mean temperature in Sodankylä during the summers of 1901, 1937 and 1972 would have been higher than in 2024 if they had occurred at today's level of global warming (Fig. 5a).

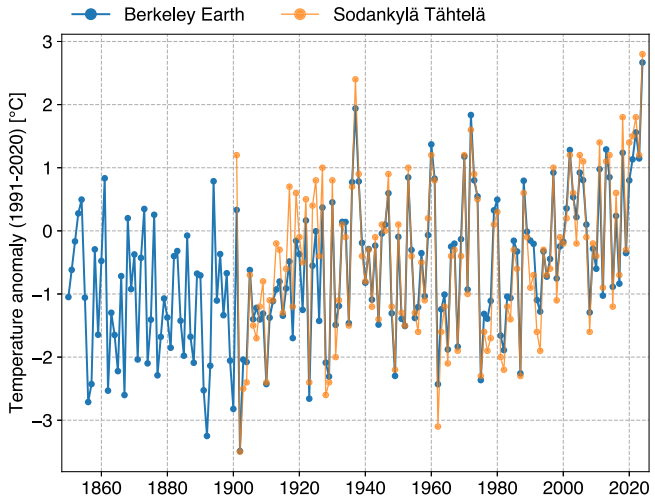

Fig. 3 | Regionally averaged summer mean temperature in northern Fennoscandia. Blue line: regionally averaged summer mean temperature anomaly in northern Fennoscandia (66°–70°N, 20°–30°E) in 1850–2024 derived from the Berkeley Earth dataset. See Fig. 1c for the used domain. Orange line shows the temperature anomaly observed in Sodankylä Tähtelä.

Then, continuous probability functions are derived from the first four moments (mean, variance, skewness, and kurtosis, annotated in Fig. 5b) of the pseudo-observation time series 1901–2024. To that end, we use stochastically generated skewed (SGS)[46] distributions, which allow for non-zero skewness and kurtosis. The SGS distributions for the 1900, 2024 and 2050 climates are illustrated in Fig. 5b. The distributions are almost identical in shape and width because the CMIP6 models simulate only small changes in local JJA mean temperature variance with global warming. However, the mean of the distributions shifts to the right due to global warming.

The observed temperature in summer 2024 (15.9 °C) is situated at the far right tail of the 1900 distribution, thus yielding an annual probability of 0.07% (5th–95th percentile range: 0.01%–0.25%). In the 2024 climate, the temperature observed in 2024 is more likely, with a probability of 6.27% (1.40%, 11.56%). From these values we derive the probability ratio (PR, Eq. 1) which describes how much more likely an event is due to climate change. We arrive at PR of 96 (19–881), meaning that climate change has made such a warm summer in Sodankylä around one hundred times more likely. The resulting PR value of 96 is about an order of magnitude higher than for individual record-warm months in Helsinki Kaisaniemi[43], but broadly comparable to PR values obtained for the summer 2018 heatwave[26,27]. The PR values for individual models are shown in Fig. S1.

The method also allows us to quantify the likelihood of observing such a high mean temperature as in 2024 under the projected climate of the 2050s. The probability is estimated at 26.62% (5.51%, 83.03%) under the shared socioeconomic pathway 2-4.5 scenario (SSP2-4.5, Fig. 5b). Thus, while a 15.9 °C summer mean temperature in Sodankylä would have been a once-in-1400-years event in the climate of 1900, it has become a once-in-16-years event in today's climate. By 2050 under the SSP2-4.5 scenario, a summer this warm is expected to occur every four years, with somewhat

Table 1 | Time coverages of the datasets and the top-5 warmest JJA periods in Sodankylä Tähtelä and in the two reconstructions. The parentheses show the average temperature

	Time coverage	1st warmest	2nd warmest	3rd warmest	4th warmest	5th warmest
Sodankylä Tähtelä	1901–2024	2024 (15.9 °C)	1937 (15.5 °C)	2018 (14.9 °C)	2022 (14.9 °C)	1972 (14.7 °C)
BJ23	850–2019 CE	1937 (15.5 °C)	2018 (15.1 °C)	2014 (14.8 °C)	2006 (14.4 °C)	1960 (14.3 °C)
MH14	−7–2010 CE	1937 (15.6 °C)	34 (15.1 °C)	1092 (15.1 °C)	891 (15.1 °C)	−3 (14.9 °C)

Fig. 4 | The confidence intervals of the reconstructions. a BJ23 reconstruction, with the red line showing the reconstructed temperature, and grey lines the 95% confidence intervals. **b** Same as (**a**), but for the MH14 reconstruction with year 34 CE highlighted. The black line in both panels shows a 30-year moving average. The blue dashed line shows the observed temperature in 2024.

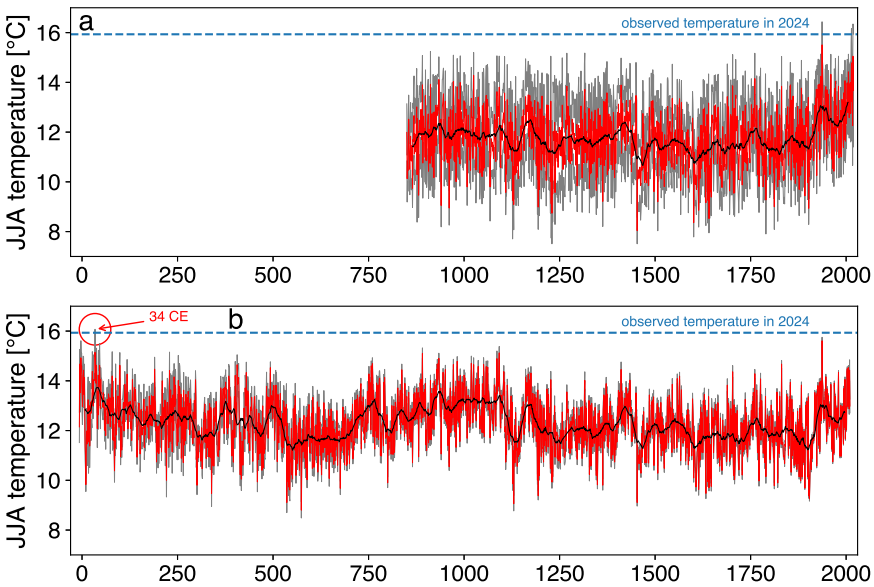

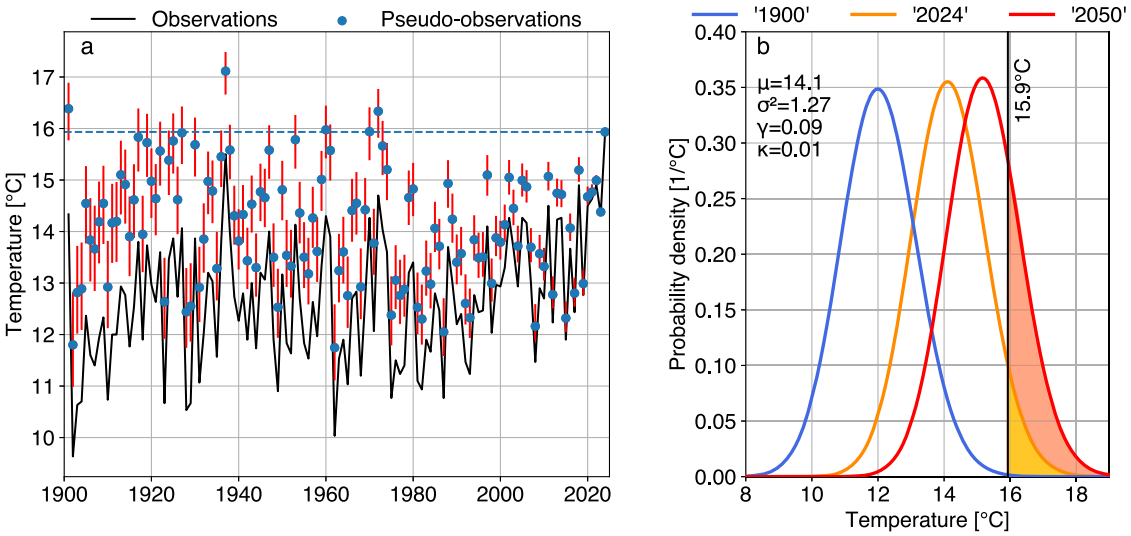

Fig. 5 | Climate change attribution results for summer 2024. a Time series of observed summer mean temperatures in Sodankylä Tähtelä in 1901–2024. Black line shows the actual observations, and blue dots show the pseudo-observations representing today's (year 2024) climate. Red error bars in pseudo-observations indicate 5th and 95th percentiles of the model ensemble. Blue-dashed line marks the 2024 summer mean temperature, 15.9 °C. **b** SGS distributions of pseudo-observations for climates representing 1900 (blue line), 2024 (orange line), and 2050 in the SSP2-4.5 scenario (red line). Black vertical line marks the observed temperature in 2024.

more frequent occurrences under the SSP5-8.5 scenario and less frequent occurrences under the SSP1-2.6 scenario (Table S1).

For the change in intensity (ΔI, see Methods), we first determine the percentile rank of the observed temperature (T_{obs} = 15.9 °C) from the 2024 distribution. Then, we identify the corresponding temperature at the same percentile in the 1900 distribution. For this, we obtain a temperature of 13.8 °C in the 1900 climate, which is 2.1 °C cooler than the observed mean temperature in 2024. This result suggests that climate change has raised the mean temperatures by approximately 2.1 °C, indicating that a new record would not have been reached without the influence of observed global warming. For individual CMIP6 models, the 5th–95th percentile range of ΔI is 1.4–2.8 °C (Fig. S1).

We repeated the attribution analysis using a regional Euro-Arctic domain (55°–80°N, 0°–50°E) and JJA mean temperature as a covariate, instead of global annual mean temperature (Fig. S2). While this approach better captures the regional forcings (e.g., changes in aerosols), regional and seasonal instead of global average also increases the internal variability of the predictor term. Nevertheless, we obtained PR = 141 (25–1494) and ΔI = 2.0 °C (1.5–2.7 °C) with this approach, which are of similar magnitude to the estimates derived using the global mean temperature as a predictor. This indicates that the choice of predictor did not strongly affect the attribution results.

For comparison, we analyzed a large set of CMIP6 models (244 realizations from 42 models, see Methods) to assess how frequently a record-warm summer occurs within the last five years (2020–2024) under the SSP2-4.5 scenario in the models. Here, we considered the data for 1900–2024, and therefore in a stable climate, record-warm summers should occur in any given five-year period with a probability of 5/125 (4%) purely by chance. However, in the CMIP6 simulations, the probability was disproportionately concentrated in the 2020 s: 35% of simulations produced a record-warm summer in at least one of the five years between 2020 and 2024, while only one of them had a record-warm summer in the first decade (1900–1909, Fig. S3). These results further indicate that the warming of the climate has significantly increased the likelihood of a record-warm summer in 2024 in northern Fennoscandia.

Atmospheric circulation in summer 2024 in northern Fennoscandia

As demonstrated in Section Instrumental and reconstructed summer temperatures in northern Fennoscandia, the summers 1937 and 2024 were the warmest on record in northern Fennoscandia. This raises the question of whether the atmospheric patterns driving these warm extremes were similar, or if the warmth in 2024 resulted from different factors than in 1937. This section investigates the atmospheric circulation patterns associated with the temperature anomalies during these summers. We largely follow the methodology of Ruosteenoja and Räisänen[47], using the 10 leading EOFs of the mean sea level pressure (MSLP) fields over northern Europe as predictors of the summer mean temperatures in northern Fennoscandia (see Methods).

Summer 2024 was associated with below-normal MSLP over most of Europe (Fig. 6a), with the greatest negative anomalies observed over Iceland and Greenland. In contrast, regions over the western mid-latitude North Atlantic and the Barents Sea had positive MSLP anomalies. The second warmest summer, JJA 1937, was characterised with a strong blocking pattern over northeastern Europe, with a ridge extending towards the British Isles (Fig. 6b). Nevertheless, similarly to JJA 2024, a low-pressure anomaly was observed over Iceland, though it was markedly weaker in 1937 than in 2024. In both years, positive MSLP anomalies were present in the east and negative anomalies in the west, indicating increased average southerly flow in northern Fennoscandia. The spatial correlation coefficient calculated for the area shown Fig. 6 (25°–75°N, −50°–50°E) between the MSLP anomalies of the two summers is 0.41, indicating a modest degree of similarity in the circulation fields. The summer North Atlantic Oscillation index, calculated following Dunstone et al. [48], was strongly positive in both 2024 and 1937 (not shown).

The regression model (i.e., the 10 leading EOFs) explained 53% of the variance in summer mean temperature in Sodankylä, corresponding to a Pearson correlation coefficient of 0.73 between observed and predicted values over the period 1901–2024 (Fig. S4). Thus, the model was far from perfect, but still explained the majority of the inter-annual variability in summer mean temperatures. Notably, the model predicted the highest summer mean temperature for 2024 (Fig. S4). However, in contrast to the 1930s, the regression residuals in 2024 and other recent years have been systematically positive, as expected for the greenhouse-gas-induced thermodynamic warming. We also applied the model to data from Karesuando and Karasjok (Fig. 1b), which produced qualitatively similar results (not shown).

The contributions of the various EOF components for JJA 2024 and 1937 temperatures are shown in Fig. 7a, b. For both summers, the dominant EOFs for the temperature are the same: EOF3 and EOF5. This indicates that

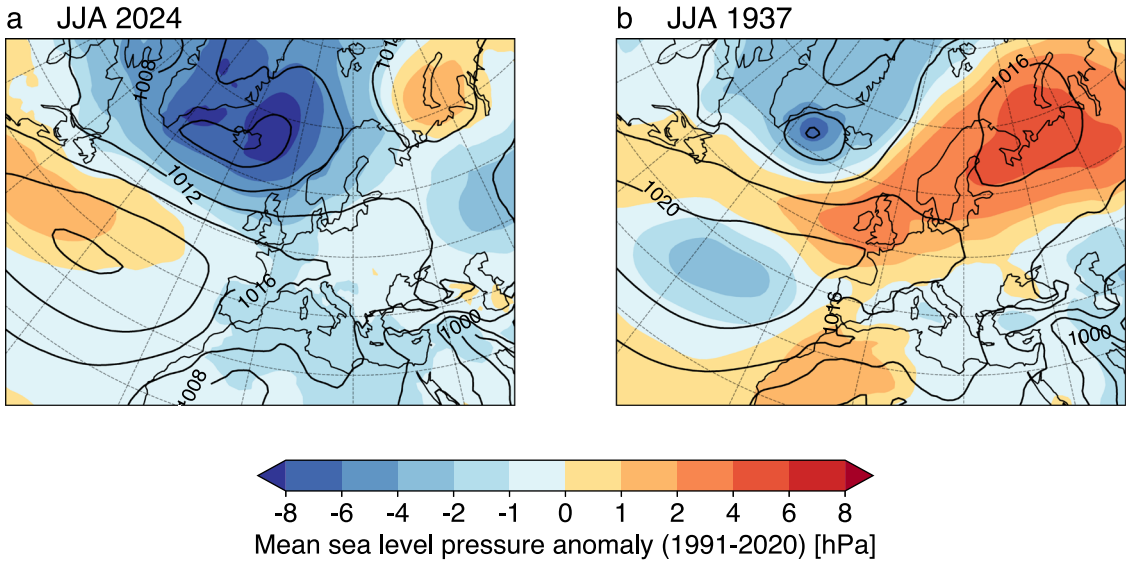

Fig. 6 | Sea level pressure fields in summer 2024 and 1937. Sea level pressure (contours) and its anomaly from the 1991–2020 average (shading) in JJA 2024 (**a**) and JJA 1937 (**b**). The 2024 data are from the ERA5 reanalysis and the 1937 data from the ERA-20C reanalysis.

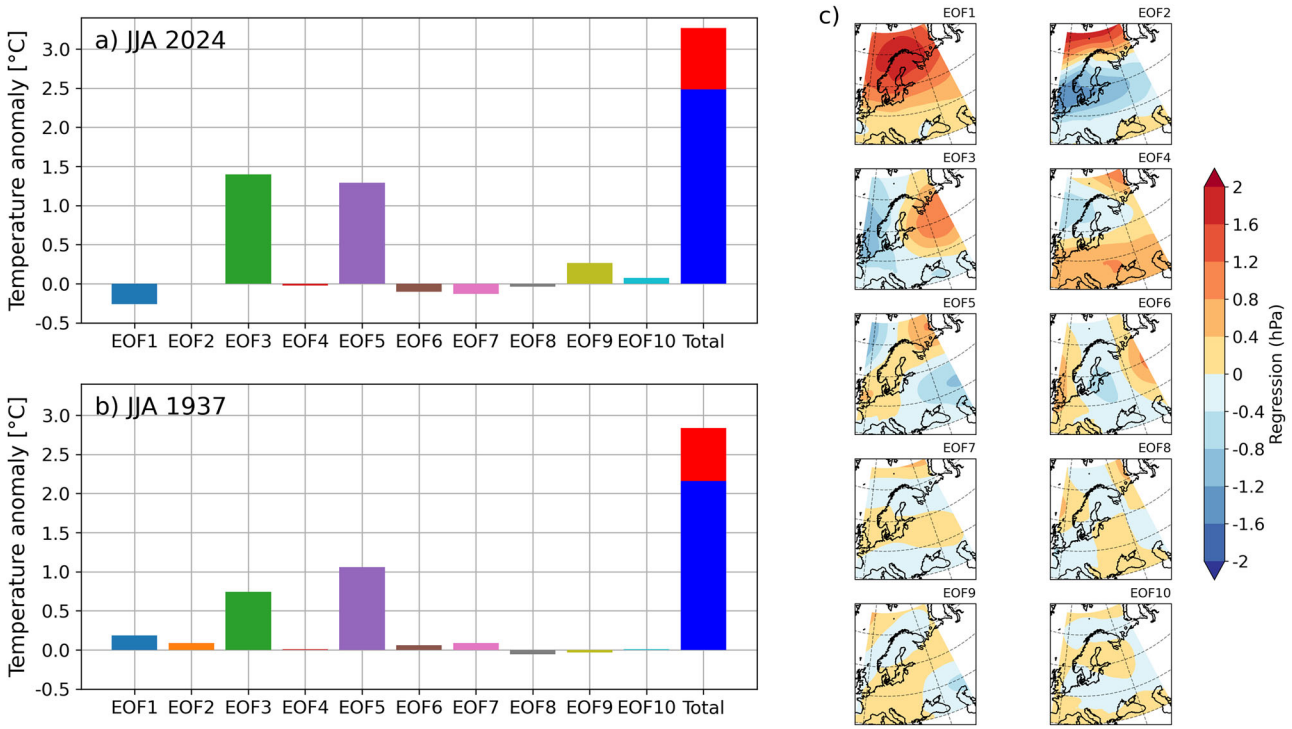

Fig. 7 | The impact of atmospheric circulation on summer mean temperatures in 2024 and 1937. Contributions of the EOF components of the regression model to the predicted temperature anomaly in Sodankylä Tähtelä in summer (**a**) 2024 and (**b**) 1937. The rightmost bar shows the total predicted temperature anomaly (blue) and the observed anomaly (red). The temperature anomalies are expressed relative to the 1901–2024 average. **c** Spatial patterns of the EOF components 1–10 of the MSLP for JJA, represented as regression of the MSLP anomaly onto the EOF indices.

the summer temperatures in both years have largely similar causes, in other words, they had mainly similar atmospheric circulation. EOF3 represents the east-west dipole in the MSLP, while EOF5 mainly reflects a local southwest-northeast oriented ridge across northwestern Europe (Fig. 7c). Thus, the high pressure pattern over the Barents Sea, as seen in both summers (Fig. 6a, b), is strongly projected on both EOF3 and EOF5 components. In summer 2024, however, the contribution of EOF3 was significantly stronger than in 1937, indicating a stronger southerly flow at Sodankylä.

To assess the influence of various EOF components on northern Fennoscandian JJA temperatures, we calculated the Pearson correlation coefficients between the EOF components and Sodankylä JJA temperatures (Table S2). The highest correlations were found for EOF3 ($R = 0.54$) and for EOF5 ($R = 0.39$), with EOF1 having statistically insignificant correlation

($R = 0.10$). Regression fields of 2-m temperature to EOF1, EOF3, and EOF5 indices reveal that EOF1, which features a blocking pattern over northern Fennoscandia, primarily affects temperature in southern Fennoscandinavia with smaller anomalies in the north (Fig. S5). EOF1 still made a positive contribution to the JJA temperature in 1937 but a negative one in 2024 (Fig. 7a, b), consistent with the positive (negative) pressure anomalies in northern Fennoscandia in 1937 (2024) (Fig. 6).

In contrast, summers with high EOF3 or EOF5 contribution, such as 2024, are typically characterized by a high pressure anomaly east of Fennoscandia and consequently higher positive temperature anomalies in northern Fennoscandia (Fig. S5). Under these conditions, warm air masses can be advected from the east or southeast (particularly in EOF3), while northern Fennoscandia experiences reduced cloud cover and increased solar radiation (Fig. S6), further enhancing the warming effect of the advection.

In summary, favourable atmospheric circulation contributed to the summer warmth both in 2024 and 1937. However, a precise attribution of the observed temperature anomaly to the circulation remains challenging due to inter-annual variability in the residual term (Fig. S4). Nevertheless, the residual term has been systematically positive in recent years, likely reflecting the influence of ongoing human-induced climate warming.

Discussion and conclusions

Despite the modern, anthropogenically forced warming during the last decades, the summer 1937 remained unprecedentedly warm in northern Fennoscandia until 2024. This has, at times, challenged the notion that current warming is exceptional, particularly in comparison to the natural climate variability over the past 2000 years. While the BJ23 reconstruction demonstrated that long-term summer warming in Fennoscandia has surpassed the natural variability of the past millennium, our study extends this finding by showing that the warmth of a single summer, namely 2024, has now also exceeded the inter-annual variability seen throughout the Common Era. This finding holds true for two independent reconstructions, derived using different methods—maximum latewood density (MH14) and wood anatomy (BJ23)—which increases the robustness of our results.

Until now, the influence of anthropogenic climate change on heat extremes in northern Fennoscandia has been inadequately demonstrated. Previous attribution studies of the summer 2018 heatwave, for example, either used a large spatial domain that included southern Fennoscandia[26] or relied on observational data 1950 onwards[27], thus excluding the warm anomaly of the 1930s. The World Weather Attribution analysis[49] used in-situ observations for Sodankylä 1908–2018 and found no robust evidence of climate change impact for the highest 3-day maximum temperature recorded in 2018, due to contrasting trends between models and observations. Indeed, there are examples of severe summer heat in northern Fennoscandia during the 20th century, such as the 1972 heatwave, which remains one of the most intense recorded in Europe[50], and the summer of 1937, which held the record as the warmest summer in northern Finland until 2024 (Figs. 1 and 3). Hence, this study is potentially the first to quantify the impact of climate change on summer heat in northern Fennoscandia using century-long in-situ observations.

Nevertheless, the attribution analysis is subject to some limitations. The pseudo-observations are generated by combining the observed global mean temperature change with CMIP6-model based regression coefficients that linearly relate the local mean and variance of temperature to global warming. However, as illustrated in Fig. 5a, the pseudo-observations for the first half of the 20th century appear to be somewhat higher than those of the past 40 years, suggesting that the models might slightly overestimate the ratio between the local and global warming.

This potential overestimation could be linked to several factors. It is well known that the 1920–1930s were warm especially in the European sector of the Arctic, including northern Fennoscandia. The reasons for this early-20th-century warming are not fully understood, but studies suggest that natural variability, together with reduced sea ice cover in the Barents Sea, was one of the leading causes[51]. However, it is unclear whether the warm Atlantic Ocean was driving the atmospheric circulation or to what extent it was the atmosphere driving the ocean[52]. It has also been suggested that the early-20th-century warming and the subsequent mid-20th-century cooling are due to changes in external forcing, especially aerosol forcing[53,54]. To better account for these regional variations, we conducted an additional attribution experiment in which we used the regional summer mean temperature as a predictor in place of the global mean temperature (Fig. S2). The results from this experiment suggest a similar contribution of climate change to the observed temperature in 2024 than that derived using the global mean temperature as a covariate. Therefore, we believe that the key results (PR = 96 and $\Delta I = 2.1$ °C) are relatively robust to the choice of predictor.

We found that the two record-warm summers, 1937 and 2024, were largely associated with similar atmospheric circulation. During these summers, both EOF3 and EOF5 components of MSLP variability were strongly positive (Fig. 7a, b), indicating high pressure anomalies over the eastern side of northern Fennoscandia. This aligns with the findings of Kim et al. [55] who showed that hot days in northern Finland are associated with a statistically significant positive pressure anomaly over Finland and its eastern surroundings. Furthermore, regression onto EOF3 and EOF5 indices shows that summers like 1937 and 2024 typically have reduced cloudiness and increased sunshine (Fig. S6). Notably, Räisänen[56] demonstrated that cloud cover variability, and especially its effect on shortwave radiation, is the main energetic driver of year-to-year summer temperature variability in northern Europe. In other words, high pressure systems are generally associated with warmer conditions due to increased solar radiation, and additional warming can result from warm air advection on the western flank of the high pressure system.

It is noteworthy that the global climate in 1937 was about 1 °C cooler than in 2024[57]. Even so, the JJA mean temperature in Sodankylä in 1937 was only 0.4 °C cooler than in 2024 (Table 1). It is therefore likely that if the atmospheric conditions during summer 1937 had occurred in 2024, the summer would have been even warmer. Our pseudo-observations suggest that in such a scenario, the summer temperature would have been approximately 1 °C higher than in 2024 (Fig. 5a). This conclusion is further supported by our EOF analysis. Specifically, EOF1, which reflects a blocking pattern over northern Fennoscandia (Fig. 7c), contributed negatively to the summer 2024 but positively to the summer 1937 (Fig. 7a). Hence, a more high-pressure-dominated weather pattern in 2024 would likely have resulted in even higher temperatures. Consequently, the extreme warmth in summer 2024 was likely not at the upper limit of what is possible in the current climate, given the right combination of atmospheric conditions.

In this paper, we employed two distinct approaches—tree-ring reconstructions and a CMIP6-based attribution method—to demonstrate the impact of anthropogenic climate change for the summer 2024 in northern Fennoscandia. We showed that summer 2024 was the warmest on record in northern Fennoscandia in the Common Era, and human-induced climate change made the warmth about 96 times more likely and about 2.1 °C warmer. Notably, summer 2024 was also record-warm in the Northern Hemisphere extratropical land areas, with a mean temperature about 0.14 °C higher than in 2023 (not shown), which was found to be the warmest in 2000 years[33].

Data and methods

Instrumental temperature data

We use monthly mean temperature observations from three weather stations: Sodankylä Tähtelä (Finland), Karesuando (Sweden) and Karasjok (Norway) station. These were obtained from Finnish Meteorological Institute, Swedish Meteorological and Hydrological Institute and Norwegian Meteorological Institute, respectively. Summer (Jun-Aug) mean temperatures were calculated from the monthly mean temperatures.

Reanalysis and gridded temperature data

We use monthly averaged MSLP, total cloud cover fraction and surface net solar radiation data for the period 1901–2010 from the ERA-20C

reanalysis[58] and for the 2011–2024 from the ERA5 reanalysis[59]. The monthly fields were used in 1° horizontal resolution.

Berkeley Earth land-only temperature dataset[60] at 1° horizontal resolution at monthly intervals was used to calculate the 2-m temperature anomalies and ranking in Figs. 1 and 3, as well as the summer temperature of the Northern Hemisphere (30–90 °N), using the same regional definition as in Esper et al. [33].

Climate model data

We use monthly mean near-surface temperature from all available realisations in Coupled Model Intercomparison Project 6 (CMIP6) ensemble. In total, 244 realisations from 42 models are analysed when calculating the distribution of record-warm summers in northern Fennoscandia for the period 1900–2024 (Fig. S3). These models are the same as those used in a previous study[61], with the exception that CanESM5 is now part of CMIP6, whereas it was treated separately in the earlier study. See Table S4 in Rantanen et al. [61] for the list of all models and the number of realisations per model.

In addition, a smaller subset (29 models, one realisation per model) of these CMIP6 models is used in the attribution method when calculating the regression coefficients (Section Climate change attribution methodology). The list of models used can be found from Fig. S1 of this study and Table S1 of Rantanen et al. [43].

Tree-ring reconstructions

We employ two previously published tree-ring based temperature reconstructions representing sites in northern Fennoscandia. The summer (June through August) temperature reconstruction based on maximum latewood density covers the period from −7 to 2010 CE[34] (referred to hereafter as MH14). This reconstruction combined the data published from the region Finnish Lapland and northernmost Sweden[38,62–65], with state-of-the-art methods to remove non-climatic effects from tree growth data. Another reconstruction we explore is based on wood anatomy. More precisely, the warm-season (May through August) temperatures were reconstructed using the delta radial-cell-wall thickness parameter that represents the difference between radial-cell-wall thickness in the latewood and earlywood, i.e., between the maximum radial-cell-wall thickness and minimum radial-cell-wall thickness[32] (referred to hereafter as BJ23). This reconstruction covers the period from 850 to 2019 CE and a region similar to MH14.

These reconstructions were scaled to summer temperatures observed at the Sodankylä Tähtelä meteorological station. This station benefits from a long history of observations as the monthly mean temperatures are available since 1901. The station has been located at almost the same site in Sodankylä throughout its history, and at exactly the same location since 1949. The station has been recognized as a Centennial Observation Station by the WMO. For more information about the station history, see Kataja[66] or Bösinger[67]. Following the methods of Esper et al. [33], tree-ring based temperatures were calibrated to instrumental data by scaling them to the mean and standard deviation of the Sodankylä temperature data. A cross-calibration/verification exercise was carried out to evaluate the relationships between the types of data over time.

The instrumental period was divided into early (1901–1955) and late (1956–2010) periods. First, the calibration of tree-ring based temperatures (i.e., scaling) was done using the early data and the data withheld from scaling was used to calculate verification statistics (the squared correlation coefficient, reduction of error, RE; coefficient of efficiency, CE)[29,68]. Second, the exercise was repeated using the late period for scaling and early period for verification. The positive RE and CE statistics, obtained for both subperiods (Table 2), indicated acceptable reconstruction skill. Finally, the scaling was performed over the full period (1901–2010) and the obtained relationships were used to scale the pre-instrumental tree-ring data to palaeoclimatic estimates of Sodankylä temperatures.

The 95% uncertainties of the reconstructions were obtained by scaling the uncertainties calculated from the spread of annual tree growth values, provided in the original publications[32,34], using the same coefficients as in the scaling of the reconstruction data.

Table 2 | Statistics over the early and late periods to verify the scaled temperatures (MH14 and BJ23) over the instrumental period

Calibration period Verification period	1901–1955 1956–2010	1956–2010 1901–1955	1901–2010
Calibration/MH14			
R^2	0.582	0.506	0.541
Verification/MH14			
R^2	0.506	0.582	
RE	0.486	0.296	
CE	0.483	0.293	
Calibration/BJ23			
R^2	0.687	0.637	0.662
Verification/BJ23			
R^2	0.637	0.687	
RE	0.634	0.580	
CE	0.632	0.578	

The squared correlation coefficient (R^2) is calculated over both subperiods, the reduction of error (RE), and coefficient of efficiency (CE) statistics over the verification period.

Climate change attribution methodology

To estimate how climate change affected (1) the probability of summer mean temperature and (2) the intensity, i.e., the mean temperature of the summer in northern Fennoscandia, we use the attribution methodology previously documented in Rantanen et al. [43].

The initial step in the process is to convert the observed time series of summer mean temperature into pseudo-observations, which represent stationary past, present, or future climates. In this study, the years 1900, 2024 and 2050, respectively, are used as the basis for these pseudo-observations. The pseudo-observations are derived on the assumption that the mean values and variability of the local summer mean temperature change linearly with the low-pass-filtered global mean temperature. The regression coefficients are derived from the same set of 29 CMIP6 models' simulations for the years 1901–2100 as in Rantanen et al. [43]. Here, the historical simulations from 1901 to 2014 are merged with the SSP2-4.5 scenario simulations for the period 2015–2100. The selection of the scenario is crucial when employing the method to estimate the probabilities of future events, but is substantially less critical for the real-time attribution of extremes where the inter-scenario differences in global warming are very modest. According to the multi-model mean regression coefficients, the mean JJA temperature in Sodankylä Tähtelä is projected to increase by 1.5 °C per degree of global warming, while temperature variance is expected to decrease by 2.6% per degree of global warming.

Subsequently, a four-parameter non-Gaussian distribution[46] using the mean, variance, skewness, and kurtosis of the sample is fitted to the pseudo-observations. We use the whole time series of pseudo-observations, i.e., from 1901 to 2024 in order to obtain a sufficient sample (> 100 years of data) to reliably estimate the probabilities near the tails of the distribution.

The uncertainty of the attribution estimates is evaluated by repeating the calculation for individual CMIP6 models and using a bootstrap sampling of internal variability for 1000 times in the pseudo-observation time series[43]. This gives us 29 × 1000 = 29,000 realisations from which we present the 5–95 percentile interval. Thus, the methodology accounts for both uncertainties arising from internal variability and model differences.

For the probability ratio (PR), we calculate the ratio between present and past probabilities:

$$PR = P\left(T \geq T_{obs}\right) / P_{cf}\left(T \geq T_{obs}\right) \quad (1)$$

Here, $P(T \geq T_{obs})$ represents the probability of temperatures of at least $T_{obs} = 15.9$ °C occurring in the current climate, obtained from the SGS

Table 3 | Cumulative variance (%) explained by the leading EOFs of MSLP and JJA temperature

EOFs included	Explained variance (MSLP, %)	Explained variance (T, %)
EOF1	41.1	0.9
EOF1-2	65.2	2.2
EOF1-3	76.3	30.8
EOF1-4	85.2	30.9
EOF1-5	91.0	46.0
EOF1-6	93.8	46.3
EOF1-7	95.1	48.0
EOF1-8	96.1	50.3
EOF1-9	97.0	52.5
EOF1-10	97.5	52.9

The MSLP EOFs are computed for the northern European domain (40–76°N, 4°W–54°E), while the temperature variance is based on JJA mean temperature from Sodankylä Tähtelä.

distribution for 2024. $P_{cf}(T \geq T_{obs})$ is the corresponding probability in a counterfactual climate with no anthropogenic influences, which is here approximated by the climate in the year 1900.

We also calculate the change in intensity (ΔI). This parameter is obtained by finding the percentile corresponding to the observed mean temperature ($T_{obs} = 15.9$ °C) from the 2024 SGS distribution, and then finding the temperature T_{cf} corresponding to the same percentile in the 1900 distribution. ΔI is then calculated from their difference:

$$\Delta I = T_{obs} - T_{cf} \quad (2)$$

Regression model for atmospheric circulation

We adopt largely the same method as in Ruosteenoja and Räisänen[47]. We use monthly mean MSLP anomaly fields computed from the dataset consisting of the ERA-20C reanalysis for the years 1901–2010 and the ERA5 reanalysis for the years 2011–2024. For homogeneity, the monthly mean differences between the two reanalyses for the years 2000–2010 were subtracted from the ERA5 MSLP fields for the years 2011–2024. The anomaly fields were calculated relative to the period 1991–2020. The choice of the anomaly baseline does not affect our results, as only relative variations in MSLP matter, and not the absolute anomaly reference.

Following Ruosteenoja and Räisänen[47], the leading 10 EOFs (explaining 97.5% of the total annual variance) of the MSLP anomalies over the JJA periods 1901–2024 in the domain 40–76°N, 4°W–54°E were selected as predictors for the regression model. The choice of 10 EOFs balanced the accuracy of the model while minimising the risk of overfitting. Table 3 lists the cumulative variance explained by the leading 10 EOFs for MSLP and Sodankylä JJA temperature.

The response variable of the regression model (i.e., the predictand) was the summer mean temperature in Sodankylä Tähtelä in 1901–2024, but as sensitivity experiments, the model was also run using summer mean temperatures at Karesuando and Karasjok.

Data availability

Station observations are available online from the Finnish Meteorological Institute (Sodankylä Tähtelä, https://en.ilmatieteenlaitos.fi/download-observations), the Swedish Meteorological Institute (Karesuando, https://www.smhi.se/data/meteorologi/ladda-ner-meteorologiska-observationer/airtemperatureInstant), and the Norwegian Centre for Climate Services (Karasjok, https://seklima.met.no/). Original time series of BJ23 and MH14 reconstructions are available at https://doi.org/10.5281/zenodo.7993298 and https://doi.org/10.25921/xbrn-p124, respectively. The MH14 and BJ23 time series scaled to Sodankylä Tähtelä station observations are available at https://doi.org/10.5281/zenodo.15172781. ERA5 data are available from Copernicus Climate Data Store at https://cds.climate.copernicus.eu. ERA-20C reanalysis data are available from the Meteorological Archival and Retrieval System (MARS) archive of European Centre for Medium-Range Weather Forecasts (ECMWF). Berkeley Earth temperature data are available from https://berkeleyearth.org/data/. CMIP6 data are available from Earth System Grid Federation (ESGF) archive at https://esgf-data.dkrz.de/search/cmip6-dkrz/.

Code availability

The Python codes needed for reproducing the results are available at https://doi.org/10.5281/zenodo.15172781[69]. The attribution method is available from GitHub: https://github.com/fmidev/cmip6-attribution/.

Received: 2 December 2024; Accepted: 13 April 2025;
Published online: 26 April 2025

References

1. Rousi, E. et al. The extremely hot and dry 2018 summer in central and northern Europe from a multi-faceted weather and climate perspective. *Nat. Hazards Earth Syst. Sci.* **23**, 1699–1718 (2023).
2. Vautard, R. et al. Human contribution to the record-breaking June and July 2019 heatwaves in Western Europe. *Environ. Res. Lett.* **15**, 094077 (2020).
3. Lhotka, O. & Kyselý, J. The 2021 European heat wave in the context of past major heat waves. *Earth Space Sci.* **9**, e2022EA002567 (2022).
4. Tripathy, K. P. & Mishra, A. K. How unusual is the 2022 European compound drought and heatwave event? *Geophys. Res. Lett.* **50**, e2023GL105453 (2023).
5. Holley, D. & Lee, S. H. Forecasting extreme heat in the UK during July 2022. *Weather* **77**, 320–321 (2022).
6. Ionita, M. et al. Examining the Eastern European extreme summer temperatures of 2023 from a long-term perspective: the role of natural variability vs. anthropogenic factors. *Nat. Hazards Earth Syst. Sci.* **24**, 4683–4706 (2024).
7. Sun, Y., Jia, G. & Xu, X. Extreme high temperatures and heatwave events across Europe in 2023. *Environ. Res. Commun.* **7**, 021001 (2025).
8. Rousi, E., Kornhuber, K., Beobide-Arsuaga, G., Luo, F. & Coumou, D. Accelerated western European heatwave trends linked to more-persistent double jets over Eurasia. *Nat. Commun.* **13**, 3851 (2022).
9. Vautard, R. et al. Heat extremes in Western Europe increasing faster than simulated due to atmospheric circulation trends. *Nat. Commun.* **14**, 6803 (2023).
10. Singh, J., Sippel, S. & Fischer, E. M. Circulation dampened heat extremes intensification over the Midwest USA and amplified over Western Europe. *Commun. Earth Environ.* **4**, 1–9 (2023).
11. Patterson, M. North-West Europe hottest days are warming twice as fast as mean summer days. *Geophys. Res. Lett.* **50**, e2023GL102757 (2023).
12. Schumacher, D. L. et al. Exacerbated summer European warming not captured by climate models neglecting long-term aerosol changes. *Commun. Earth Environ.* **5**, 1–14 (2024).
13. Yin, Z., Dong, B., Wei, W. & Yang, S. Anthropogenic impacts on amplified midlatitude European summer warming and rapid increase of heatwaves in recent decades. *Geophys. Res. Lett.* **51**, e2024GL108982 (2024).
14. Dong, B. & Sutton, R. T. Drivers and mechanisms contributing to excess warming in Europe during recent decades. *Npj Clim. Atmos. Sci.* **8**, 1–13 (2025).
15. Copernicus. C3S seasonal lookback: summer 2024. https://climate.copernicus.eu/c3s-seasonal-lookback-summer-2024 (2024).
16. Patterson, M., Befort, D. J., O'Reilly, C. H. & Weisheimer, A. Drivers of the ECMWF SEAS5 seasonal forecast for the hot and dry European summer of 2022. *Q. J. R. Meteorol. Soc.* **150**, 4969–4986 (2024).

17. Ionita, M. & Nagavciuc, V. 2024: the year with too much summer in the eastern part of Europe. *Weather* (2025).
18. FMI. August and summer were exceptionally warm in Lapland. https://en.ilmatieteenlaitos.fi/press-release/5YqDjNb07wMCOKuYjBn8x8 (2024).
19. YLE. *Frozen North no More: Hotter Summers Set Lapland Ablaze* https://yle.fi/a/74-20107279 (*News*, 2024).
20. Stott, P. A., Stone, D. A. & Allen, M. R. Human contribution to the European heatwave of 2003. *Nature* **432**, 610–614 (2004).
21. Zachariah, M. et al. *Without Human-Caused Climate Change Temperatures of 40°C in the UK Would Have Been Extremely Unlikely*. https://hdl.handle.net/10289/16234 (2022).
22. Philip, S. et al. *Extreme April Heat in Spain, Portugal, Morocco & Algeria Almost Impossible without Climate Change*. http://hdl.handle.net/10044/1/103833 (2023).
23. Kornhuber, K., Bartusek, S., Seager, R., Schellnhuber, H. J. & Ting, M. Global emergence of regional heatwave hotspots outpaces climate model simulations. *Proc. Natl. Acad. Sci. USA* **121**, e2411258121 (2024).
24. Sinclair, V. A., Mikkola, J., Rantanen, M. & Räisänen, J. The summer 2018 heatwave in Finland. *Weather* **74**, 403–409 (2019).
25. Wilcke, R. A. I. et al. The extremely warm summer of 2018 in Sweden – set in a historical context. *Earth Syst. Dyn.* **11**, 1107–1121 (2020).
26. Yiou, P. et al. Analyses of the Northern European summer heatwave of 2018. *Bull. Am. Meteorol. Soc.* **101**, S35–S40 (2020).
27. Leach, N. J. et al. Anthropogenic influence on the 2018 summer warm spell in Europe: the impact of different spatio-temporal scales. *Bull. Am. Meteorol. Soc.* **101**, S41–S46 (2020).
28. Tejedor, E. et al. Recent heatwaves as a prelude to climate extremes in the western Mediterranean region. *Npj Clim. Atmos. Sci.* **7**, 1–7 (2024).
29. Fritts, H. C. *Tree Rings and Climate*. (Academic Press, New York, 1976).
30. Wilson, R. et al. Last millennium northern hemisphere summer temperatures from tree rings: Part I: the long term context. *Quat. Sci. Rev.* **134**, 1–18 (2016).
31. Anchukaitis, K. J. et al. Last millennium Northern Hemisphere summer temperatures from tree rings: Part II, spatially resolved reconstructions. *Quat. Sci. Rev.* **163**, 1–22 (2017).
32. Björklund, J. et al. Fennoscandian tree-ring anatomy shows a warmer modern than medieval climate. *Nature* **620**, 97–103 (2023).
33. Esper, J., Torbenson, M. & Büntgen, U. 2023 summer warmth unparalleled over the past 2000 years. *Nature* **631**, 94–97 (2024).
34. Matskovsky, V. V. & Helama, S. Testing long-term summer temperature reconstruction based on maximum density chronologies obtained by reanalysis of tree-ring data sets from northernmost Sweden and Finland. *Clim* **10**, 1473–1487 (2014).
35. Sigl, M. et al. Timing and climate forcing of volcanic eruptions for the past 2,500 years. *Nature* **523**, 543–549 (2015).
36. Rinne, J. & Alestalo, M. Volcanic impacts dominate bidecadal-multidecadal temperature variations during the late holocene in northern fennoscandia. *J. Geophys. Res. Atmospheres* **124**, 11661–11671 (2019).
37. Ogurtsov, M., Lindholm, M., Jalkanen, R. & Veretenenko, S. V. North Atlantic sea surface temperature, solar activity and the climate of Northern Fennoscandia. *Adv. Space Res.* **59**, 980–986 (2017).
38. Esper, J. et al. Orbital forcing of tree-ring data. *Nat. Clim. Change* **2**, 862–866 (2012).
39. Berger, A. & Loutre, M. F. Insolation values for the climate of the last 10 million years. *Quat. Sci. Rev.* **10**, 297–317 (1991).
40. Esper, J., Düthorn, E., Krusic, P. J., Timonen, M. & Büntgen, U. Northern European summer temperature variations over the Common Era from integrated tree-ring density records. *J. Quat. Sci.* **29**, 487–494 (2014).
41. Matskovsky, V. & Helama, S. Direct transformation of tree-ring measurements into palaeoclimate reconstructions in three-dimensional space. *Holocene* **26**, 439–449 (2016).
42. Helama, S. et al. Disentangling the evidence of Milankovitch forcing from tree-ring and sedimentary records. *Front. Earth Sci.* **10**, 871641 (2022).
43. Rantanen, M., Räisänen, J. & Merikanto, J. A method for estimating the effect of climate change on monthly mean temperatures: September 2023 and other recent record-warm months in Helsinki, Finland. *Atmos. Sci. Lett.* **25**, e1216 (2024).
44. Räisänen, J. & Ruokolainen, L. Estimating present climate in a warming world: a model-based approach. *Clim. Dyn.* **31**, 573–585 (2008).
45. Räisänen, J. & Ruokolainen, L. Ongoing global warming and local warm extremes: a case study of winter 2006-2007 in Helsinki, Finland. *Geophysica* **22**, 45–65 (2008).
46. Sardeshmukh, P. D., Compo, G. P. & Penland, C. Need for caution in interpreting extreme weather statistics. *J. Clim.* **28**, 9166–9187 (2015).
47. Ruosteenoja, K. & Räisänen, J. Evolution of observed and modelled temperatures in Finland in 1901–2018 and potential dynamical reasons for the differences. *Int. J. Climatol.* **41**, 3374–3390 (2021).
48. Dunstone, N. et al. Skilful predictions of the Summer North Atlantic Oscillation. *Commun. Earth Environ.* **4**, 1–11 (2023).
49. WWA. Heatwave in northern Europe, summer 2018. https://www.worldweatherattribution.org/attribution-of-the-2018-heat-in-northern-europe/ (2018).
50. Russo, S., Sillmann, J. & Fischer, E. M. Top ten European heatwaves since 1950 and their occurrence in the coming decades. *Environ. Res. Lett.* **10**, 124003 (2015).
51. Bengtsson, L., Semenov, V. A. & Johannessen, O. M. The early twentieth-century warming in the arctic—a possible mechanism. *J. Clim.* **17**, 4045–4057 (2004).
52. Hegerl, G. C., Brönnimann, S., Schurer, A. & Cowan, T. The early 20th century warming: Anomalies, causes, and consequences. *WIREs Clim. Change* **9**, e522 (2018).
53. Booth, B. B. B., Dunstone, N. J., Halloran, P. R., Andrews, T. & Bellouin, N. Aerosols implicated as a prime driver of twentieth-century North Atlantic climate variability. *Nature* **484**, 228–232 (2012).
54. Haustein, K. et al. A limited role for unforced internal variability in twentieth-century warming. *J. Clim.* **32**, 4893–4917 (2019).
55. Kim, S., Sinclair, V. A., Räisänen, J. & Ruuhela, R. Heat waves in Finland: present and projected summertime extreme temperatures and their associated circulation patterns. *Int. J. Climatol.* **38**, 1393–1408 (2018).
56. Räisänen, J. Energetics of interannual temperature variability. *Clim. Dyn.* **52**, 3139–3156 (2019).
57. WMO. WMO confirms 2024 as warmest year on record at about 1.55°C above pre-industrial level. *World Meteorological Organization* https://wmo.int/media/news/wmo-confirms-2024-warmest-year-record-about-155degc-above-pre-industrial-level (2025).
58. Poli, P. et al. ERA-20C: an atmospheric reanalysis of the twentieth century. *J. Clim.* **29**, 4083–4097 (2016).
59. Hersbach, H. et al. The ERA5 global reanalysis. *Q. J. R. Meteorol. Soc.* **146**, 1999–2049 (2020).
60. Rohde, R. A. & Hausfather, Z. The Berkeley earth land/ocean temperature record. *Earth Syst. Sci. Data* **12**, 3469–3479 (2020).
61. Rantanen, M. et al. The Arctic has warmed nearly four times faster than the globe since 1979. *Commun. Earth Environ.* **3**, 1–10 (2022).
62. Schweingruber, F. H., Bartholin, T., Schaur, E. & Briffa, K. R. Radiodensitometric-dendroclimatological conifer chronologies from Lapland (Scandinavia) and the Alps (Switzerland). *Boreas* **17**, 559–566 (1988).
63. Briffa, K. R. et al. A 1,400-year tree-ring record of summer temperatures in Fennoscandia. *Nature* **346**, 434–439 (1990).
64. Grudd, H. Torneträsk tree-ring width and density ad 500–2004: a test of climatic sensitivity and a new 1500-year reconstruction of north Fennoscandian summers. *Clim. Dyn.* **31**, 843–857 (2008).
65. Melvin, T. M., Grudd, H. & Briffa, K. R. Potential bias in 'updating' tree-ring chronologies using regional curve standardisation: re-processing

1500 years of Torneträsk density and ring-width data. *Holocene* **23**, 364–373 (2013).
66. Kataja, E. A short history of the Sodankylä geophysical observatory. *Geophysica* **35**, 3–13 (1999).
67. Bösinger, T. The geophysical observatory in Sodankylä, Finland – past and present. *Hist. Geo- Space Sci.* **12**, 115–130 (2021).
68. Briffa, K. R., Jones, P. D., Pilcher, J. R. & Hughes, M. K. Reconstructing Summer Temperatures in Northern Fennoscandinavia Back to A.D. 1700 Using Tree-Ring Data From Scots Pine. *Arct. Alp. Res.* **20**, 385–394 (1988).
69. Rantanen, M. Data and Python scripts to produce the results in 'Summer 2024 in northern Fennoscandia was very likely the warmest in 2000 years'. https://doi.org/10.5281/zenodo.15172781 (2025).

Acknowledgements

This research has been supported by the ACCC Flagship funded by the Academy of Finland (decision no 337552) and the RESICLIM, CLAIMS, FIRST and WELT projects funded by the Academy of Finland (decisions no 342890, 362263, 339788 and 355268). We acknowledge the World Climate Research Programme, which is responsible for CMIP6. We thank the climate modelling groups for making available their model output, the Earth System Grid Federation (ESGF) for archiving the data and providing access, and the multiple funding agencies who support CMIP6 and ESGF. ECMWF and Copernicus Climate Change Service are acknowledged for making ERA-20C and ERA5 data available.

Author contributions

M.R. made the figures and wrote the first draft of the manuscript. S.H. produced the tree-ring reconstructions and contributed to writing the sections related to these data. J.R. developed the attribution methodology and provided guidance on both the attribution and circulation analysis. H.G. secured funding for the study. All authors reviewed, commented and approved the final manuscript.

Competing interests

The authors declare no competing interests.

Additional information

Supplementary information The online version contains supplementary material available at https://doi.org/10.1038/s41612-025-01046-4.

Correspondence and requests for materials should be addressed to Mika Rantanen.